Registration for Orthopaedic Interventions

Ziv Yaniv

1 Introduction

Registration is the process of computing the transformation that relates the coordinates of corresponding points given in two different coordinate systems. It is one of the key components in orthopaedic navigation guidance and robotic systems. Most commonly, registration is used to transfer preoperative information to the intraoperative setting and for assessment of postoperative results. Slightly less common uses include the use of registration to facilitate automated procedure planning, and computation of population atlases which are later used for intraoperative registration. The standard mathematical formulation of a registration algorithm is as an optimization task, where a problem specific quantity is minimized or maximized. This formulation implies that in most cases registration does not have an analytic solution and therefor we are not guaranteed that the obtained result is the optimal value (minimum or maximum).

The majority of texts describing registration only focus on algorithmic aspects. In this work we aim to provide a holistic view that we believe benefits both clinical practitioners and system developers. We therefore introduce the concept of a registration framework. That is, we consider both the algorithmic aspects and the integration of the algorithm into the clinical workflow as it pertains to data acquisition and possible effects on clinical outcome.

When evaluating a registration framework it is beneficial to use a theoretical construct, the ideal clinical registration framework. This framework is evaluated using five criteria and has the following characteristics:

1. Accuracy and precision: sub-millimetric target registration error throughout the working space, with sub-millimetric precision.

Ziv Yaniv
TAJ Technologies Inc. and Office of High Performance Computing and Communications, National Library of Medicine, National Institutes of Health, Bethesda, MD, 20894, USA, e-mail: zivyaniv@nih.gov

2. Robustness: not effected by errors and outliers in the input data (e.g. low image quality, user localization errors).
3. Computation speed: takes less than 1sec to complete the computation.
4. Obtrusiveness: no registration specific hardware is introduced into the environment (e.g. US machine used only for registration), and input data is easily acquired in less than 10sec to yield a streamlined workflow.
5. Clinical side effects: has no detrimental side effects (e.g. registration requires additional exposure to ionizing radiation from imaging, additional incisions or surgical procedures).

From an engineering or scientific standpoint the important evaluation criteria of a registration framework are those directly associated with the registration algorithm, the first three criteria listed above. As a result, the later two criteria often do not receive sufficient attention, resulting in sub-optimal clinical registration frameworks. This is readily evident when analyzing the registration framework of one of the earliest robotic systems used in orthopaedics. The ROBODOC system for total hip replacement initially utilized a paired-point registration algorithm to align the robot to the patient. The engineers designing the registration framework placed most of the emphasis on the registration algorithm, choosing to use an optimal algorithm that provides high accuracy and precision, is robust and computes the result in less than 1sec. Unfortunately, while the registration algorithm was optimal, the framework was not. In this case, the system used implanted fiducials to define the points used for registration. This required an additional minor intervention prior to surgery. More importantly, it resulted in significant collateral damage, patients suffered from persistent severe knee pain due to nerve damage caused by the pin implantation [82]. We therefore encourage developers of registration algorithms to consider the whole registration framework and not just the algorithm, as this is what ultimately determines clinical acceptance.

Before we delve into descriptions of specific registration algorithms we will highlight a fundamental characteristic of the errors associated with rigid registration. Spatial errors become larger as one moves farther from the reference frame's origin. This is primarily of importance to operators of such systems, providing the theoretical explanation to observations in the field such as those described in [97]. As we are dealing with rigid registration, we have errors both in the estimated translation and rotation. The translation errors have a uniform effect throughout space and do not depend on the location of the origin. The rotational errors, on the other hand, have a spatially varying effect that is dependent on the distance from the origin, this is sometimes referred to as the "lever effect". Thus, for the same rotational error a point that is close to the origin will exhibit a smaller spatial error as compared to a point that is farther away from the origin.

From a practical standpoint we cannot mitigate the effect of translational errors, but we can mitigate the effect of rotational errors. That is, if we place the origin of our reference frame in the center of the spatial region of interest, we minimize the maximal distance to the origin and thus minimize the maximal spatial error. Figure 1 illustrates these observations in the planar case.

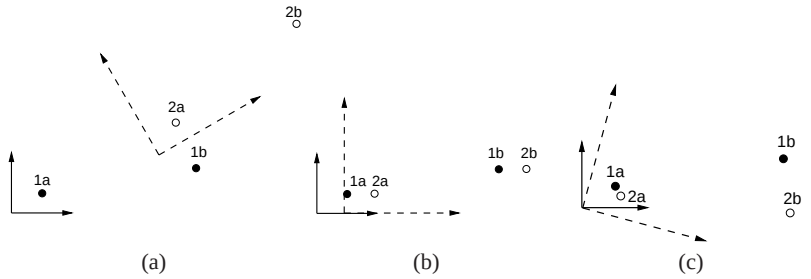

Fig. 1 Characteristics of rigid registration spatial errors: (a) corresponding points (1a-2a, 1b-2b) before registration; after registration (b) error only in translation, (c) error only in rotation. In both cases it is clear that registration reduced the spatial error between the points. It is also clear that the effect of the translational error on the spatial errors is uniform throughout space, while the effect of the rotational error depends on the distance from the origin. In theory, one can eliminate the effect of rotational errors for a single point by placing the origin of the reference frame at this point of interest.

While developers of registration frameworks strive to construct the ideal framework, this is not an easy task. More importantly, it is context dependent. For example, introducing an US machine for the sole purpose of registration makes the framework non-ideal. On the other hand, if the US machine is already available, for instance to determine breaches in pedicle screw hole placement [52], utilizing it for registration purposes does not preclude the framework from being considered ideal.

Given that constructing the ideal framework is hard, it is only natural that developers of guidance systems have devised schemes that bypass this task. We therefor start our overview of registration in orthopedics with approaches that perform registration implicitly.

2 Implicit Registration

We identify two distinct approaches to performing implicit registration. The first combines preoperative calibration with intraoperative volumetric image acquisition using cone-beam CT (CBCT). The second uses patient specific templates that are physically mounted onto the patient in an accurate manner. These devices physically constrain the clinician to planned trajectories for drilling or cutting.

2.1 Intraoperative CBCT

This approach relies on the use of a tracked volumetric imaging system to implicitly register the acquired volume to a Dynamic Reference Frame (DRF) rigidly attached to the patient. During construction of the imaging device, it is calibrated such that

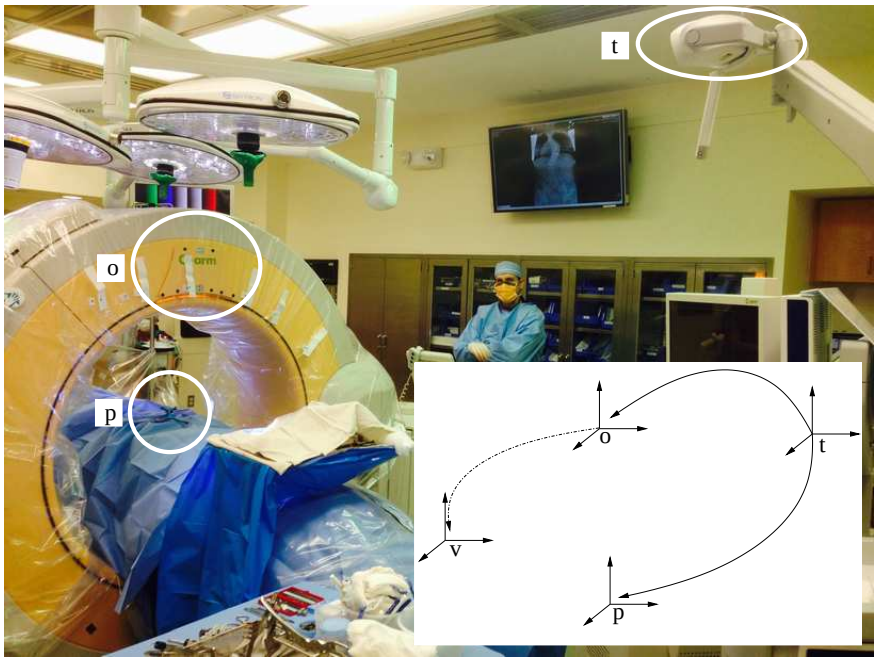

Fig. 2 The O-arm system from Medtronic (Minnisota, MN, USA) facilitates implicit registration via factory calibration. Picture shows the clinical setup (courtesy of Dr. Matthew Oetgen, Children's National Health System, USA). Inset shows corresponding coordinate systems and transformations. Transformations from tracking coordinate system, t, to patient DRF, p, and O-arm DRF, o, vary per procedure and are obtained from the tracking device. The transformation between the O-arm DRF, o, and the volume coordinate system acquired by the O-arm, v, is fixed and obtained via factory calibration. Once the volume is acquired intraoperatively it is implicitly registered to the patient as the transformation from the patient to the volume is readily constructed by applying the three known transformations.

the location and orientation of the reconstructed volume is known with respect to a DRF that is built into the system. Intraoperatively, a volumetric image is acquired while the patient's DRF and imaging device's DRF are both tracked by a spatial localization system. This allows the navigation system to correctly position and orient the volume in physical space. It should be noted that some manufacturers refer to this registration bypass as automated registration, although strictly speaking the system is not performing intraoperative registration. Figure 2 shows an example of the physical setup and coordinate systems involved in the use of such a system.

These systems have been used to guide various procedures for a number of anatomical structures including the hip [11, 118], the foot [101], the tibia [134], the spine [23, 38, 83, 107, 53], and the hand [115].

When compared to our ideal registration framework these systems satisfy almost all requirements. They are accurate and precise with submillimetric performance. They are robust, although the use of optical tracking devices means that they are

dependent on an unobstructed line of sight both to the patient's and device's DRFs. They provide the desired transformation in less than 1sec, as almost no computation is performed intraoperatively after image acquisition. These systems are not obtrusive as they are used to acquire both intraoperative X-ray fluoroscopy and volumetric imaging. The one criterion where they can be judged as less than ideal is that these systems expose the patient to ionizing radiation.

While these systems offer many advantages when evaluated with regard to components of the registration framework, they do have other limitations. The quality of the volumetric images acquired by these devices is lower than that of diagnostic CT images and this can potentially have an effect on the quality of the visual guidance they provide. Obviously, one can register preoperative diagnostic images (CT, PET, MR) to the intraoperative CBCT, but this changes the registration framework and it is unclear whether such a system retains the advantages associated with the existing one. Another, non technical, disadvantage is the cost associated with these imaging systems. They do increase the overall cost of the navigation system. One potential approach to addressing the cost of high end CBCT systems is to retrofit non-motorized C-arm systems to perform CBCT reconstructions. This requires that the position and orientation of the C-arm be known for each of the acquired X-rays during a manual rotation. Two potential solutions to this task have been described in the literature. The C-Insight system from Mazor Robotics (Caesarea, Israel) [134] uses an intrinsic tracking approach. It both calibrates the X-ray system and estimates the C-arm pose using spherical markers visible in the X-ray images. An extrinsic approach to tracking is describe in [2]. This system utilizes inertial measurement units attached to a standard C-arm to obtain the pose associated with each image. As both approaches retrofit standard C-arms the quality of the reconstructed volumes is expected to be lower than those obtained with motorized CBCT machines, as these also utilize flat panel sensors which yield higher quality input for CBCT reconstruction.

2.2 Patient specific templates

This approach relies on the use of physical templates to guide cutting or drilling. The templates are designed based on anatomical structures and plans formulated using preoperative volumetric images, primarily diagnostic CT. This is in many ways similar to stereotactic brain surgery, using patient mounted frames. To physically guide the surgeon the template incorporates two components, the bone contact surface which is obtained via segmentation from the preoperative image and guidance channels which correspond to the physical constraints specified by the plan. Templates can be created either via milling, subtractive fabrication, or via 3D printing, additive fabrication. The later approach has become more common as the costs of 3D printers have come down. Figure 3 illustrates this concept in the context of pedicle screw insertion.

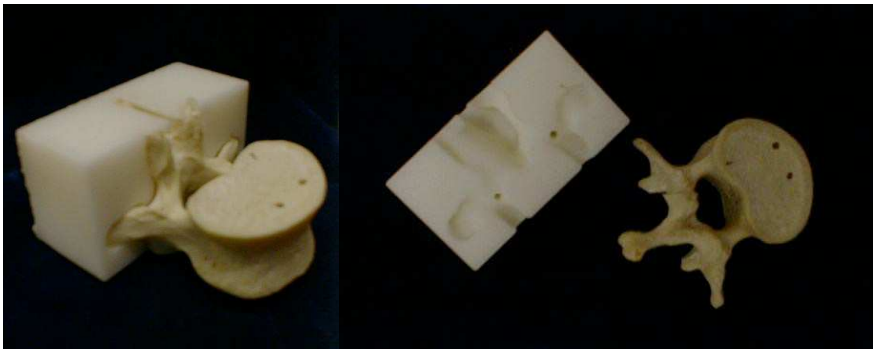

Fig. 3 Patient specific 3D printed template for pedicle screw insertion. Template incorporates drill trajectories planned on preoperative CT (courtesy Dr. Terry S. Yoo, National Institutes of Health, USA).

Patient specific templates have been used to guide various procedures for a number of anatomical structures including the spine [15, 68, 69, 98], the hand [60, 70, 85], the hip [41, 98, 119, 148], and the knee [43, 98].

When compared to the ideal registration framework, this approach provides sufficient accuracy, precision and robustness. Registration is obtained implicitly in an intuitive manner, as the template is manually fit onto the bone surface. This approach is not obtrusive as it does not require additional equipment other than the template. In theory there are no clinical side effects associated with the use of a template. Unfortunately, achieving accuracy, precision and robustness requires that the template fit onto the bone in a unique configuration. This potentially requires a larger contact surface, resulting in larger incisions than those used by standard minimally invasive approaches [119]. While a smaller contact surface is desirable it should be noted that this will potentially increase the chance that the operator ”fits the square peg into a round hole” (e.g. wrong-level fitting for pedicle screw insertion).

3 3D/3D registration

In orthopaedics, 3D/3D registration is utilized for alignment of preoperative data to the physical world, spatial alignment of data as part of procedure planning, and for construction of statistical shape and appearance models with the intent of replacing the use of preoperative CT for navigation with a patient specific model derived from the statistical one.

Alignment of preoperative data to the physical world is the most common usage of registration in orthopaedics. It has been described as a component of robotic procedures applied to the knee [7, 78, 67, 79, 96, 103], and hip [73, 81, 109]. In the context of image-guided navigation, it has been described as a component of

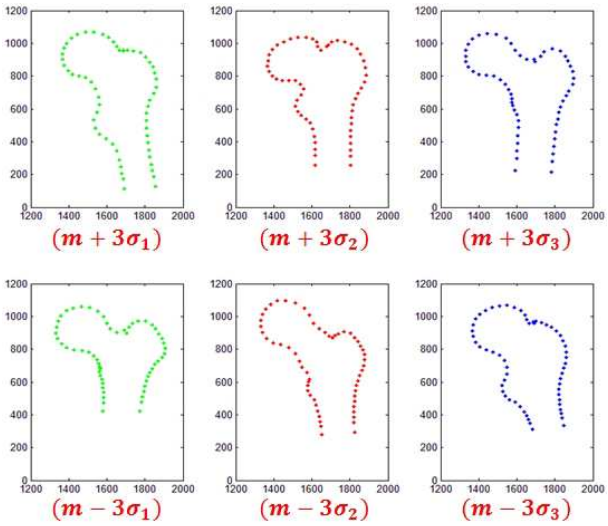

Fig. 4 2D proximal femur statistical point distribution model, three standard deviations from the mean shape, along the first three modes of variation (courtesy Dr. Guoyan Zheng, University of Bern, Switzerland).

procedures in the hip [8, 9, 10, 54, 61, 94, 110, 118, 119], the femur [8, 16, 94, 99, 154], the knee [54, 99, 116], and the spine [31, 46, 61, 100, 120, 143].

In the context of planning, 3D/3D registration has been used for population studies targeting implant design [58], for the selection and alignment of a patient specific optimal femoral implant in total hip arthroplasty [90], and for planning the alignment of multiple fracture fragments using registration to the contralateral anatomy, thus enabling automated formulation of plans in distal radius osteotomy [27, 28, 102, 111], humerus fracture fixation [14, 35], femur fracture fixation [86] and potentially for scaphoid fracture fixation [63].

In the context of statistical model creation, the first journal publications to describe the use of statistical shape models in orthopedics were [34] and [117]. The motivation for this work was to create a patient specific model for guiding ACL reconstruction and total knee arthroplasty without the need of a preoperative 3D scan. A statistical point distribution model of the distal part of the femur was created by digitizing the surfaces of multiple dry bone specimens and creating the required anatomical point correspondence via non-rigid 3D/3D registration. Many others follow a similar approach but with one primary difference, the models used to describe the population are obtained from previously acquired 3D scans, CT or MR, of other patients. This allows modeling of both shape and intensity. For a detailed overview of the different aspects of constructing statistical shape models we refer the interested reader to [44].

In orthopedics, statistical shape models that use registration for establishing anatomical point correspondences have primarily used the free-form deformation

method proposed in [104] and the diffeomorphic-demons method proposed in [131]. These registration methods were utilized for creating models of the femur, pelvis and tibia [9, 16, 58, 108, 137, 147]. This approach was also recently applied in 2D, using 2D/2D registration to establish point correspondences for a proximal femur model [140]. Figure 4 shows the resulting 2D statistical point distribution model.

At this point we would like to highlight two aspects associated with the use of statistical point distribution models which one should always think about: does the input to the statistical model truly reflect the population variability (e.g. using femur data obtained only from females will most likely not reflect the shape and size of male femurs); and if point correspondences were established using registration, how accurate and robust was the registration method.

Having motivated the utility of 3D/3D registration in orthopedics, we now turn our attention to several common algorithms, pointing out their advantages and limitations.

3.1 Point set to point set registration

In this section we discuss three common algorithm families used to align point sets in orthopedics, paired-point algorithms, surface based algorithms and statistical surface models.

Paired-point algorithms use points with known correspondences to compute the rigid transformation between the two coordinate systems. In this setting points are localized, most often, manually both in image space via mouse clicks, and in physical space via digitizing using a tracked calibrated pointing device such as described in [122]. Both calibration and tracking of pointer devices can be done with sub-millimetric accuracy.

In general, we are given three or more corresponding points in two Cartesian coordinate systems:

$$\mathbf{x_{li}} = \widehat{\mathbf{x_{li}}} + \mathbf{e_{li}}$$
$$\mathbf{x_{ri}} = \widehat{\mathbf{x_{ri}}} + \mathbf{e_{ri}}$$

where $\widehat{\mathbf{x_{li}}}, \widehat{\mathbf{x_{ri}}}$ are the true point coordinates related via a rigid transformation $T(\widehat{\mathbf{x_{li}}}) = \widehat{\mathbf{x_{ri}}}$, $\mathbf{x_{li}}, \mathbf{x_{ri}}$ are the observed coordinates, and $\mathbf{e_{li}}, \mathbf{e_{ri}}$ are the errors in localizing the points.

The most common solution to this problem is based on a least squares formulation:

$$T^* = \underset{T}{\operatorname{argmin}} \sum_{i=1}^{n} \|\mathbf{x_{ri}} - T(\mathbf{x_{li}})\|^2$$

The solution to this formulation is optimal if we assume that there are no outliers and that the Fiducial Localization Errors (FLE)[1] follow an isotropic and homoge-

[1] In this context the term fiducial is used to denote a point used to compute the registration, be it an artificial marker or anatomical landmark.

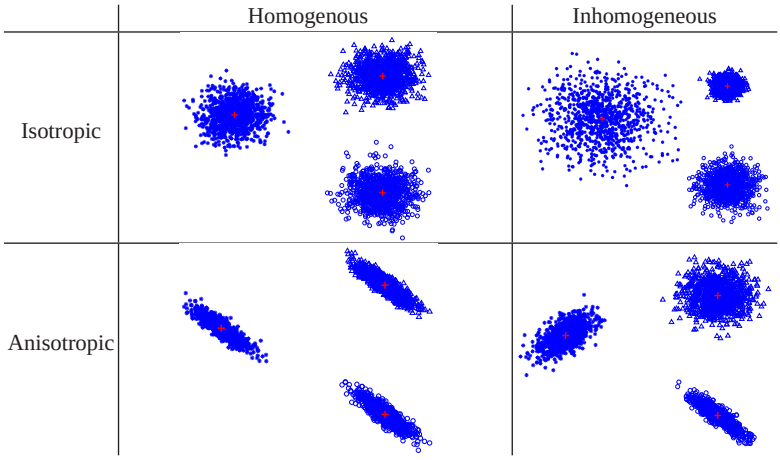

Fig. 5 Categories of fiducial localization error according to their variance. Plus (red) indicates fiducial location and star/circle/triangle marks (blue) denote localization variability.

nous Gaussian distribution. That is, the error distribution is the same in all directions and is the same for all fiducials. Figure 5 visually illustrates the possible FLE categories.

While the formulation is unique, several analytic solutions have been described in the literature, with the main difference between them being the mathematical representation of rotation. These include use of a rotation matrix [3, 128], a unit quaternion [32, 47], and a dual quaternion [132]. All of these algorithms guarantee a correct registration if the assumptions hold. Luckily, empirical evaluation has shown that all choices yield comparable results [30].

In practice, FLE is often anisotropic, such as when using optical tracking systems, where the error along the camera's viewing direction is much larger than the errors perpendicular to it [138]. In this case, the formulation described above does not lead to an optimal solution. Iterative solutions addressing anisotropic-homogenous noise and anisotropic-inhomogeneous noise models were described in [77] and [84] respectively. These methods did not replace the least squares solutions even though they explicitly address the true error distributions. This is possible due to two attributes of the original algorithms, they are analytic, that is they do not require an initial solution as iterative algorithms do, and they are extremely easy to implement. Case in point, Table 1 is a fully functioning implementation of the method described in [128] using MATLAB (The Mathworks Inc., Natick, MA, USA).

One of the issues with paired-point registration methods is that the pairing is explicit, that is the clinician has to indicate which points correspond. This is often performed as part of a manual point localization process which is known to be inaccurate both in the physical and the image spaces [46, 112]. The combination of fixed pairing and localization errors reduces the accuracy of registration, as we are not truly using the same point in both coordinate systems. If on the other hand we

```
function T = absoluteOrientation(pL, pR)

n = size(pL,2);
meanL = mean(pL,2);
meanR = mean(pR,2);
[U,S,V] = svd((pL - meanL(:,ones(1,n))) *
              (pR - meanR(:,ones(1,n)))');
R = V*diag([1,1,det(U*V)])*U';
t = meanR - R*meanL;

T = [R, t; [0, 0, 0, 1]];
```

Table 1 Source code shows complete implementation of analytic paired point rigid registration in MATLAB. The analytic nature of the solution and the simplicity of implementation make it extremely attractive for developers, even though this solution assumes noise is isotropic and homogenous, which is most often not the case.

allow for some flexibility in matching points then we may improve the registration accuracy. This leads directly to the idea of surface based registration.

Preoperative surfaces are readily obtained from diagnostic CT. Intraoperative surface acquisition is often done using a tracked pointer probe [4]. To ensure registration success one must acquire a sufficiently large region so that the intraoperative surface cannot be ambiguously matched to the preoperatively extracted one. This is a potential issue if it requires increased exposure of the anatomy only for the sake of registration. A possible non-invasive solution is to use calibrated and tracked ultrasound (US) for surface acquisition. US calibration is still an active area of research with multiple approaches described in the literature [76], most yielding errors on the millimeter scale. More recently published results report sub-millimetric accuracy [80]. Once the tracked calibrated US images are acquired, the bone surface is segmented in the images and its spatial location is computed using the tracking and calibration data. Automated segmentation of the bone surface is not a trivial task. In the works described in [8] and [9] the femur and pelvis were manually segmented in the US images prior to registration, this is not practical for clinical use. Automated bone surface segmentation algorithms in US images have been described in [57, 54, 100, 110, 120] for B-mode US and in [79] for A-mode. These algorithms were evaluated as part of registration frameworks which have clinically acceptable errors (on the order of 2mm).

Surface based registration algorithms use points *without* a known correspondences to compute the rigid transformation between the two coordinate systems. A natural approach for scientists tackling such problems is to decompose them into sub problems with the intent of using existing solutions for each of the sub problems. This general way of thinking is formally known as ”computational thinking” and is a common approach in computer science [139].

Given that we have an analytic algorithm for computing the transformation when we have a known point pairing it was only natural for computer scientists to propose a two step approach towards solving this registration task. First match points based

on proximity and then estimate the transformation using the existing paired-point algorithm. This process is repeated iteratively with the incremental transformations combined until the two surfaces are in correspondence. This algorithmic approach is now known as the Iterative Closest Point (ICP) algorithm. This algorithm was independently introduced by several groups [13, 20, 149].

While the simplicity of the ICP algorithm makes it attractive, from an implementation standpoint, it has several known deficiencies. The final solution is highly dependent on the initial transformation estimate, and speed is dependent on the computational cost of point pairing. In addition, the use of the analytic least squares algorithm to compute the incremental transformations assumes that there are no outliers and that the error in point localization is isotropic and homogenous. Many methods for improving these deficiencies have been described in the literature, with a comprehensive summary given in [105]. One aspect of the ICP algorithm that was not addressed till recently was that the localization errors are often anisotropic and inhomogeneous. A variant of ICP addressing this issue was recently described in [72].

From a practical standpoint, a combination of paired-point and an ICP variant is often used. The analytic solution most often provides a reasonable initialization for the ICP algorithm which then provides improved accuracy. This was shown empirically in [46]. Unfortunately, this combination still does not guarantee convergence to the correct solution. This is primarily an issue when the intraoperatively digitized surface is small when compared to the preoperative surface. In this situation the surface registration may be trapped by multiple local minima. This is most likely the reason for the poor registration results reported in [4] for registering the femur head in the context of hip arthroscopy.

Statistical surface model based registration [34, 117] are similar to surface based registration as described above, but with one critical difference, they do not use patient specific preoperative data. Instead of a patient specific surface obtained from CT, a surface model is created and aligned to the intraoperative point cloud. The statistical model encodes the variability of multiple example bone surfaces and uses the dominant modes of variation to fit a patient specific model to the intraoperative point cloud. An advantage of using such an approach is that models created from the atlas are limited to the variations observed in the data used to construct it. Thus, these models are plausible. Unfortunately, they often will not provide a good fit to previously unseen pathology. This can be mitigated by allowing the model to locally deform in a smooth manner to better fit the intraoperative point cloud [117].

3.2 Intensity based registration

Intensity based registration aligns two images by formulating the task as an optimization problem. The optimized function is dependent on the image intensity values and the transformation parameters. As the intensity values for the images are given at a discrete set of grid locations and the transformation is over a contin-

uous domain, registration algorithms must interpolate intensity values at non grid locations. This means that all intensity based registration algorithms include at least three components: (1) The optimized similarity function which indicates how similar are the two images, subject to the estimated transformation between them; (2) An optimization algorithm; and (3) an interpolation method.

A large number of similarity measures have been described in the literature and are in use. Selecting a similarity measure is task dependent with no ”best” choice applicable to all registration tasks. The selection of a similarity measure first and foremost depends on the relationship between the intensity values of the modalities being registered. When registering data from the same modality one may use the sum of squared differences or the sum of absolute differences. For modalities with a linear relationship between them one may use the normalized cross correlation. For modalities with a general functional relationship one can use the correlation ratio. Finally, for more general relationships, such as the probabilistic relationship between CT and PET one may use mutual information or normalized mutual information. These last similarity measures assume the least about the two modalities and are thus widely applicable. This does not mean that they are optimal, as we are ignoring other relevant evaluation criteria: computational complexity, robustness, accuracy, and convergence range. Incorporating domain knowledge when selecting a similarity measure usually improves all aspects of registration performance. More often than not, selecting a similarity measure should be done in an empirical manner, evaluating the selection on all relevant criteria. Case in point, the study of similarity measures described in [92] for 2D/3D registration of X-ray/CT.

Optimization is a mature scientific field with a large number of algorithms available for solving both constrained and unconstrained optimization tasks [33]. The selection of a specific optimization method is tightly coupled to the characteristics of the optimized function. For example, if the similarity measure is discontinuous using gradient based optimization methods is not recommended.

Finally, selecting an interpolation method is dependent on the density of the original data. If the images have a high spatial sampling, we can use simpler interpolation methods as the distance between grid points is smaller. With current imaging protocols linear interpolation often provides sufficiently accurate estimates in a computationally efficient manner. Obviously, other higher order interpolation methods can provide more accurate estimates with a higher computational cost [62].

In orthopedics 3D/3D intensity based non-rigid registration has been used for creating point matches for point distribution based statistical atlases. These models encode the variability of bone shape via statistics on point locations across the population. This in turn assumes that the corresponding points can be identified in all datasets. For sparse anatomically prominent landmarks this can potentially be done manually. For the dense correspondence required to model anatomical variability this is not an option. If on the other hand we non-rigidly align the volumetric data we can propagate a template mesh created from one of the volumes to the others, implicitly establishing the dense correspondence. In [9] this is performed using the free-form deformation registration approach with normalized mutual information as the similarity measure. In [16] and [108] registration is performed with a

diffeomorphic-demons method with the former using a regularization model which is tailored for improving registration of the femur. It should be noted that the demons set of algorithms assume the intensity values for corresponding points are the same for the two modalities. Finally, in [58] registration is performed using the free-form deformation algorithm and the sum of squared differences similarity measure.

Another setting in which 3D/3D intensity based rigid registration has been utilized in orthopedics is for alignment of preoperative data to the physical world, using intraoperative tracked and calibrated US to align a preoperative CT. In [94] both the US and CT images are converted to probability images based on the likelihood of a voxel being on the bone surface, with the similarity between the probability images evaluated using the normalized cross correlation metric. In [36] and [61] simulated US images are created from the CT based on the current estimate of the US probe in the physical world. In both cases simulation of US from CT follows the model described in [135]. Registration is then performed using the Covariance Matrix Adaptation Evolution Strategy, optimizing the correlation ration in the former work and a similarity measure closely related to normalized cross correlation in the later work. In [141, 142] course localization of the bone surface is automatically performed both in the CT and US with the intensity values in the respective regions used for registration using the normalized cross correlation similarity measure. To date, US based registration has not become part of clinical practice. This is primarily due to the fact that US machines are not readily available in the operating room as part of current orthopedic procedures. Requiring the availability of additional hardware only for the sake of registration appears to limit adoption of this form of registration.

We now shift our focus to the second form of registration which is relevant for orthopedics, 2D projection (X-ray) to 3D (CT/model/atlas) registration.

4 2D projection/3D

In orthopaedics 2D X-ray to 3D registration is utilized for alignment of preoperative data to the physical world, and for postoperative evaluation, primarily implant pose estimation. We divide our discussion in two, registration methods that use fiducials or implants and those that use anatomical structures. The former methods are easier to automate and are often more robust and accurate as they use man made structures specifically designed to yield accurate registration results. A broad overview of the literature describing various anatomy based registration approaches, not specific to orthopedics, was recently given in [75]. We refer the reader interested in more detailed algorithm descriptions to that publication.

We start by highlighting two aspects of 2D/3D registration which are often not described in detail in publications but effect the accuracy and success of registration: (1) Calibration of the X-ray device; and (2) in the case of anatomy based registration, how was the registration initialized.

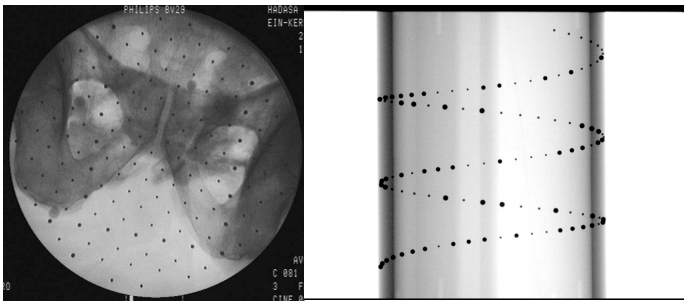

Fig. 6 Calibration images used for (left) two tier pattern for online calibration (right) helical pattern for offline calibration.

X-ray imaging devices are modeled as a pinhole camera, with distortion when the sensor is an image-intensifier, and without distortion when using a flat panel sensor. By performing calibration we estimate the geometric properties of the imaging system. These are later used by the registration algorithm to simulate the imaging process or to compute geometric information that is dependent on the geometry of the imaging apparatus. We identify two forms of calibration, online which means that calibration is carried out every time an image is acquired [12, 45, 65, 121, 150] and, offline which means calibration is carried out once and we assume the apparatus will return to the same pose whenever an image is acquired [21, 22, 24]. Both forms of calibration image a phantom with known geometry and compute the geometric properties of the imaging apparatus using the phantom's geometry and its appearance in the image. Figure 6 shows X-ray images of online and offline calibration phantoms.

The online approach is more commonly used when working with image-intensifier based C-arms that are manually manipulated. The offline approach is used when working with systems that also provide cone-beam CT functionality. That is, they are motorized and can be accurately manipulated. In the context of registration, the offline calibration has an advantage over the online approach, the image content is not occluded by the calibration phantom and thus may lead to more accurate registration results. In addition if these systems use flat-panel sensors calibration does not have to include estimation of distortion parameters, with the physical world modeled more closely by the theoretical pinhole model. Finally, if you have worked with a system that utilizes online calibration you may not have noticed the extent of the occlusion introduced by the calibration phantom. This is because many of these systems identify the occluded regions and interpolate the image information so that under visual inspection it appears as if the calibration markers are not there. In practice these images contain less information that is useful for registration than equivalent images without occlusion.

All algorithms that perform anatomy based registration are iterative. That is, they require an initial estimate of the pose of the 3D object being registered. Once the X-ray images of the anatomy are acquired the algorithm is initialized using one of several initialization approaches. The most common methods are:

1. Manual initialization - the operator manipulates the pose of the 3D object using the keyboard and mouse while the X-ray generation process is simulated using the geometric properties of the imaging system. The user manipulates the transformation parameters with the goal of making the simulated image as similar as possible to the real one. A similar, yet clinically more appropriate approach, is to use gestures observed by a depth sensor (e.g. Microsoft Kinect), or a tracking system to manipulate the 3D object [37].
2. Coarse paired point registration - use the paired-point registration algorithm described above with coarsely localized points in the intraoperative setting. Anatomical or fiducial points are localized either with a tracked and calibrated pointer or via stereo triangulation when multiple X-ray images are available.
3. Clinical setup - the geometry of the intra-operative imaging apparatus is used to bound the transformation parameters. Rough initialization can be obtained by using the intersection point of all principle rays to position the preoperative image [37]. Additionally, the specific patient setup (e.g. supine), and orientation of the X-ray images (e.g. Anterior-Posterior) can be used to constrain the transformation parameters [87]. This can be refined using a brute force approach [88]. Grid sampling the parameter space in the region around the estimate defined by the clinical setup, evaluating the similarity measure's value at each of the grid points and selecting the best one.

Additional less common approaches include an estimate based on the Fourier slice theorem [17] for X-ray/CT registration and the use of a virtual marker [130] to re-register a CT to X-ray with a process that requires an initial paired point registration with wide field of view X-rays with re-registration enabling the use of narrow field of view X-rays.

4.1 Algorithm classification

We start our overview of 2D/3D registration algorithms by identifying six classes of algorithms, a variation on the classification proposed in [75]. The classification is based on the information utilized by the algorithm, features, intensity, or gradients, and the spatial domain in which optimization is carried out ,2D or 3D.

Feature based algorithms use either anatomical surfaces or markers in 3D and anatomical edges and markers in 2D to formulate the optimization task. This requires segmentation of both 3D and 2D data, something that is not trivial to perform without introducing outliers. This is primarily an issue with the 2D intraoperative X-ray images that often include edges arising from medical equipment associated with the procedure. Using the geometric properties of the X-ray device, either: (1) the features in 3D are projected onto the 2D image and the distance between 2D features and projected features is minimized. We call this approach F2D; (2) the features in 2D are backprojected, defining rays from the camera to the feature location and the distance between the 3D surface points and the backprojected rays is minimized or another option is to identify rays arising from the same 3D feature in

multiple images, intersect them to define a 3D point and then minimize the distances between the point clouds. We call this approach F3D.

Intensity based algorithms directly use the intensity values of the images and do not require accurate segmentation, overcoming the main deficiency of feature based algorithms. Using the geometric properties of the X-ray device, either: (1) the 3D image or atlas is used to simulate an X-ray image and the similarity between the actual X-rays and the simulated ones is maximized. This similarity can be between the 2D gradients, edges, or intensity values. This is the most common registration method. In the past, the computational cost of simulating X-rays, also known as Digitally Reconstructed Radiographs (DRRs), was prohibitive. Currently this is no longer an issue, as the use of high performance Graphical Processing Units (GPU) has become commonplace and efficient creation of DRRs on the GPU is both fast and cost effective [29, 126]. We call this approach I2D; (2) the X-ray images are used in a reconstruction framework, similar to cone-beam CT. Either algebraic reconstruction or filtered backprojection methods can be used to perform reconstruction. The reconstructed volume is then rigidly registered to the preoperative volume using 3D/3D intensity based registration algorithms. The main deficiency of this approach is that it requires more X-ray images than any other method, exposing the patient to higher levels of ionizing radiation. Therefor this approach has not garnered much acceptance beyond its original proponent [125]. We call this approach I3D.

Gradient based algorithms directly use the gradients computed in 2D and 3D. This is a middle ground between intensity based registration that does not require segmentation and feature based registration which does. While this approach is interesting from an academic standpoint it has not been widely adopted, limited to the original proponents of the approach [66, 74, 124]. Using the geometric properties of the X-ray device, either: (1) the 3D gradients are projected onto the 2D image and the distance and orientation between the 2D gradients and the projected ones is minimized. We call this approach G2D; (2) the 2D gradients are backprojected and combined to form 3D estimates and the distance and orientation between the reconstructed gradients and those arising from the 3D image are minimized. We call this approach G3D.

We start our overview with methods that are based on the alignment of manufactured objects, fiducials or implants.

4.2 Fiducials and Implants

One of the simplest methods for establishing the 3D pose of a manufactured object is to attach fiducial markers to it. Often these are spherical markers that are readily detected in X-ray images. Using a calibrated X-ray device it is straightforward to create a set of backprojected 3D rays, emanating from the location of the X-ray source and going through the marker locations in the X-ray image. By using two or more images the rays corresponding to the same markers are intersected and this

Fig. 7 2D/3D registration setup used by the Mazor Robotics Renaissance system, physical setup and X-ray fluorscopy (courtesy Ms. Stephani Shipman and Dr. Doron Dinstein, Mazor Robotics, Israel): (a) X-ray calibration phantom, and (b) Pose estimation phantom. Both phantoms consist of metal spheres in known spatial configurations. Inset on the left shows a detailed view of the pose estimation phantom.

intersection point is the 3D location of the marker. Once we have the 3D locations of three or more fiducials we can compute the pose using the paired-point registration algorithm. It should be noted that this approach is not specific to orthopedics and has been described in multiple publications [25, 40, 133, 144, 145]. Given the registration jig used by the robotic spine surgery system described in [113, 114] it is highly likely that this is the registration approach in use, although the publications do not provide the specific details. Figure 7 shows the robot and pose estimation clamp in clinical use. These approaches fall into the F3D category.

Using markers from a single image to estimate the pose of an object is also possible. When we have multiple 2D-3D point correspondences this is the well known perspective-n-point (PnP) camera pose determination problem from computer vision [42]. The problem is solved by minimizing the distances between the 2D points and the projections of the 3D model points. In [146] a drill guide with embedded spherical markers was attached to a robot, enabling the estimation of the robot pose, guiding it to a final pose for performing femoral distal nailing. An evaluation study of the effect of X-ray dose on the accuracy of this form of registration was described in [39]. It was found that increasing X-ray dose increased 2D localization accuracy and the registration accuracy, but only up to a certain point. This approach falls into the F2D category.

More complex marker configurations for estimating the pose of a C-arm have also been described. One such device that has been used in the orthopedic setting is the FTRAC fiducial [49]. This is a complex marker constructed of multiple line segments, ellipses and points. The spatial configuration of these components enables the use of a single image to estimate the marker pose in 3D. In the original work the components of the marker were segmented in the X-ray image and the distance between these points and the projection of the marker components in the given pose was minimized, an F2D approach. This assumes that the segmentation in the image

was successful. In subsequent work done in the context of femoral bone augmentation surgery citeotake2012b, the need for segmentation was eliminated. Instead of using the 2D coordinates of the geometric entities, the CAD model of the marker was used to generate a simulated X-ray. The 3D pose of the marker was then estimated by comparing the simulated X-ray to the actual one, with the correct pose being the one that minimizes the difference between the simulated and actual image. This process was formulated as an optimization task, with similarity between images determined using mutual information and optimization performed with the Nelder-Mead Downhill Simplex algorithm, an I2D approach. Finally, in [51] only the point markers from the FTRAC were segmented and used in a maximum likelihood framework to estimate the fiducial's pose without requiring an explicit point correspondence between the 3D model and its 2D projection, an F2D approach.

Implants are not specifically designed to facilitate 2D/3D registration, but knowledge of their geometry, their accurate CAD model, is either available from the manufacturer or can be readily measured. This knowledge enables accurate registration as it allows for fast simulation of the X-ray imaging process with highly accurate localization of the implant edges in the simulated image.

In the context of postoperative assessment for total knee arthroplasty, registration was used to assess the relative position of the femoral and tibial implants [71]. The implant CAD models are aligned based on single fluoroscopy image. The optimal alignment is based on minimizing the distance between the 2D edges observed in the X-ray and those created by projecting the CAD model using the known X-ray geometry. A similar approach is described in [56] with the main difference being the use of two images instead of one. In both cases the approach can be classified as an F2D approach. Finally, a method that registers both the implants and femur and tibia to a pair of X-rays using a I2D approach is described in [55]. In this case the edges in the X-ray images are enhanced by a diffusion process so that they extend beyond their actual location. The pose of the implants and boney structures is estimated by generating DRRs, performing edge detection in the DRR and then maximizing the normalized cross correlation between the resulting edge image and the processed X-ray edge image.

In the context of postoperative assessment for total hip replacement, registration was used to assess the cup orientation. In [18, 19] cup and stem orientation are obtained using an I2D approach, aligning the CAD models to a single X-ray. The CAD models of the implants are used in conjunction with a refined DRR generation framework which incorporates both the geometry and material characteristics of the implants to generate the DRR. Comparison between the X-ray and DRR is based on the sum of squared differences between gradient magnitudes, optimized using a Gauss-Newton method. In [50] a similar approach is taken although with a less refined methodology for generating the DRR. Most likely this is why the DRR and X-ray image are compared using mutual information. This is a more forgiving similarity measure which only assume there is a statistical relationship between the two images accommodating less accurate simulations from a physics standpoint.

4.3 Anatomy based

Registration of anatomical structures using 2D/3D registration is more challenging than registration of fiducials or implants, as the anatomical structures often do not have unique features (e.g. femur shaft) and have higher variability than implants.

In the context of spine surgery, 2D/3D registration has been previously studied extensively [93, 106, 123]. Newer developments have been described in [88, 89] where registration is used to identify vertebral levels in a single X-ray with the intent of reducing wrong site surgery. Preoperatively, the vertebra are identified in the patient's CT. Intraoperatively, DRRs are generated using the GPU and compared with the X-ray using a gradient based similarity measure that is optimized using the Covariance Matrix Adaptation Evolution Strategy (CMA-ES). This method falls into the I2D category. A recent extension of this method to use two images evaluated the effect of angle difference between the images on the accuracy of the registration [129]. Results showed that even with small angular differences of 10-20 degrees registration errors were less than 2mm. In [64] the vertebra are registered by generating a DRR from the preoperative CT and performing edge detection on it. Edges are also detected in the X-ray and the overlap between the edges in the DRR and X-ray serves as the similarity measure which is maximized.

In the context of femur related interventions, 2D/3D registration was used for kinematic analysis in [127]. The patient's CT was aligned to a single X-ray image by generating DRRs, performing edge detection on the DRR and X-ray image with the goal of maximizing the overlap between the edges, with optimization performed using a genetic algorithm. This method falls into the I2D category. In [87] registration between the preoperative CT and 2-4 X-ray images is performed. DRRs are generated on the GPU and the gradient-information similarity measure is optimized using the CMA-ES algorithm, a classical I2D approach.

While the classical 2D/3D registration problem relies on patient specific data, aligning two datasets from the same patient, a number of groups have investigated the use of a statistical shape model instead of a 3D dataset. This is of interest as it replaces the need for acquiring a preoperative CT, reducing costs, reducing radiation exposure to the patient, and an enabling technology when a CT is not available [5, 6, 48, 152]. In [5, 6, 152] reconstruction of proximal and distal femur surface model is performed using a statistical shape model and two X-ray images. In this framework the patient specific shape is both created and aligned to the X-ray images. The framework uses a two step approach, first project the current model's surface points onto the X-ray image using the known geometric properties of the imaging device and match them with edges detected on X-ray. This defines a matching between the 3D model's surface points and the edges in the X-ray. Then compute the distance between the backprojected rays defined by the edges in the X-ray and their matched 3D surface point. The goal of optimization is to create and align a surface model which minimizes this distance. The differences between the various algorithms are primarily in the 2D matching phase. In addition the approach described in [152] includes one final step, a regularized shape deformation. That is, it allows for modification of the last shape obtained from the statistical model. This accounts

for the fact that the shape model reflects the variation of the data used to create it. On the one hand this ensures that the patient specific models created are plausible but on the other hand they are limited to be similar to past observations. By adding this final step the resulting patient specific model is both plausible and accommodates previously unseen minor variations in shape. A related approach that uses a statistical appearance model, encoding both shape and intensities was described in [48]. The femur surface and orientation is estimated using the statistical model and 3-5 images. The process is based on generating DRRs using the current estimated intensity model and pose, then matching edge points between the DRRs and X-ray images via 2D/2D nonrigid registration. Once the matches are established the distance between backprojected rays computed from the X-ray and corresponding 3D model surface points defines the distance between the model and X-ray. This distance is minimized to obtain the final femur surface model and pose.

In the context of total hip replacement 2D/3D registration has been used for postoperative evaluation. In [95] the patient's preoperative CT scan is aligned to a single X-ray image using the intensity based registration approach described in [93]. The CAD model of the cup is manually aligned using a graphical user interface. In [153, 151] cup orientation is estimated from the alignment estimated in the postoperative X-ray and registration of the patient's preoperative CT to the X-ray, without requiring a CAD model. In this case registration is performed in two steps. First anatomical landmarks in the CT and X-ray are manually defined. An initial registration is performed using an iterative solution to the PnP problem, similar to the fiducial based approach described above. This is then followed by an intensity based registration step, which compares the generated DRRs with the X-ray using a similarity measure derived from Markov random field theory. This work was later extended, replacing the second step relying on a patient specific CT with the use of a statistical shape model [155]. This second registration step follows a similar framework to the spastical shape models described above for aligning the femur.

5 Evaluation

From an academic standpoint registration is evaluated for its accuracy and speed. Accuracy is evaluated by establishing a "gold standard" with methods that are clinically not applicable, such as implanting markers to enable the use of methods that are known to be highly accurate (i.e. paired-point fiducial registration) [136]. As we have already noted at the beginning of this chapter this form of evaluation does not address all clinical aspects that determine whether a method will be clinically practical.

To enable comparison of algorithms this "gold standard" needs to be made publicly available. One of the few settings where these gold standards have been made available is in the context of 2D/3D registration [59, 91, 123].

It should be noted that the only registration algorithm with a fully developed theory predicting expected errors and their distribution is the paired-point rigid reg-

istration [26]. All other algorithms do not have a solid mathematical error prediction theory. But is this clinically relevant? The answer is, yes! This is a safety issue. If we can theoretically bound the errors then we can ensure the patients safety. On the other hand all of the evaluation methods make assumptions which may be violated in the clinical setting. For instance, most algorithms assume that the tracked reference frame is rigidly attached to the patient during data acquisition. If someone inadvertently moves the frame during data acquisition, no amount of mathematical analysis will be able to bound the registration error introduced by this unexpect act.

We would thus like to enumerate the aspects of registration which all practitioners should keep in mind:

1. Registration errors vary spatially. As long as the expected error at the specific target(s) is sufficiently low one can use the result.
2. Analytical algorithms guarantee an optimal result - as long as their assumptions are met.
3. Iterative algorithms, the majority of registration algorithms, require an initial estimate of the registration parameters. They do not guarantee an optimal result, as they depend on this initial estimate to be sufficiently close to the optimal one.
4. Assumptions made in the lab are sometimes not met in the clinic.
5. A registration result remains valid only if its assumption remain valid too (i.e. reference frame is rigidly attached to the patient).

We therefor recommend that after any registration performed in the clinic, one validate the results, and that this also be done periodically during the intervention to ensure that the registration is still valid. This is a patient safety issue which can have potentially serious repercussions [1].

6 Conclusion

Registration is a key technical technology in navigation and can serve as a tool for preoperative planning and postoperative evaluation. A large number of algorithms have been proposed and have shown clinical utility. In some cases algorithms have not made it into clinical use due to integration issues with existing clinical practices.

For developers of registration algorithms we need to remember that the goal is to integrate our algorithms into clinical practice, a task that requires additional research in terms of workflow analysis in the clinic. Designing our algorithms so that they provide a streamlined workflow and do not require the introduction of additional registration specific hardware.

For practitioners using registration algorithms it is important to understand what are the expectations of the registration algorithm and what are its limitations. Providing the expected environment and input to the algorithm should yield accurate and useful results without the need for repeated data acquisition, something that is not uncommon in the clinic.

In the end the goal of both developers and practitioners is to provide improved healthcare in a safe manner. This goal can only be attained by collaboration and knowledge sharing between the two groups.

References

[1] (2014) Class 2 Device Recall Spine & Trauma 3D 2.0. URL http://www.accessdata.fda.gov/scripts/cdrh/cfdocs/cfres/res.cfm?id=125729
[2] Amiri S, Wilson DR, Masri BA, Anglin C (2014) A low-cost tracked C-arm (TC-arm) upgrade system for versatile quantitative intraoperative imaging. International Journal of Computer Assisted Radiology and Surgery 9(4):695–711
[3] Arun KS, Huang TS, Blostein SD (1987) Least-squares fitting of two 3-D point sets. IEEE Trans Pattern Anal Machine Intell 9(5):698–700
[4] Audenaert E, Smet B, Pattyn C, Khanduja V (2012) Imageless versus image-based registration in navigated arthroscopy of the hip: a cadaver-based assessment. J Bone Joint Surg Br 94(5):624–629
[5] Baka N, Kaptein BL, de Bruijne M, van Walsum T, Giphart JE, Niessen W, Lelieveldt BPF (2011) 2D-3D shape reconstruction of the distal femur from stereo X-ray imaging using statistical shape models. Medical Image Analysis 15(6):840–850
[6] Baka N, de Bruijne M, van Walsum T, Kaptein BL, Giphart JE, Schaap M, Niessen WJ, Lelieveldt BPF (2012) Statistical shape model-based femur kinematics from biplane fluoroscopy. IEEE Trans Med Imag 31(8):1573–1583
[7] Banger M, Rowe PJ, Blyth M (2013) Time analysis of MAKO RIO UKA procedures in comparision with the Oxford UKA. Bone Joint J 95-B(Supp 28):89
[8] Barratt DC, Penney GP, Chan CSK, Slomczykowski M, Carter TJ, Edwards PJ, Hawkes DJ (2006) Self-calibrating 3D-ultrasound-based bone registration for minimally invasive orthopedic surgery. IEEE Trans Med Imag 25(3):312–323
[9] Barratt DC, Chan CSK, Edwards PJ, Penney GP, Slomczykowski M, Carter TJ, Hawkes DJ (2008) Instantiation and registration of statistical shape models of the femur and pelvis using 3D ultrasound imaging. Medical Image Analysis 12(3):358–374
[10] Beaumont E, Beaumont P, Odermat D, Fontaine I, Jansen H, Prince F (2011) Clinical validation of computer-assisted navigation in total hip arthroplasty. Adv Orthop p 171783
[11] Behrendt D, Mütze M, Steinke H, Koestler M, Josten C, Böhme J (2012) Evaluation of 2D and 3D navigation for iliosacral screw fixation. International Journal of Computer Assisted Radiology and Surgery 7(2):249–255

[12] Bertelsen A, Garin-Muga A, Echeverria M, Gomez E, Borro D (2014) Distortion correction and calibration of intra-operative spine X-ray images using a constrained DLT algorithm. Comput Med Imaging Graph 38(7):558–568
[13] Besl PJ, McKay ND (1992) A method for registration of 3D shapes. IEEE Trans Pattern Anal Machine Intell 14(2):239–255
[14] Bicknell RT, et al (2007) Early experience with computer-assisted shoulder hemiarthroplasty for fractures of the proximal humerus: development of a novel technique and an in vitro comparison with traditional methods. J Shoulder Elbow Surg 16(3 Suppl):S117–S125
[15] Birnbaum K, Schkommodau E, Decker N, Prescher A, Klapper U, Radermacher K (2001) Computer-assisted orthopedic surgery with individual templates and comparison to conventional operation method. Spine 26(4):365–370
[16] Blanc R, Seiler C, Székely G, Nolte L, Reyes M (2012) Statistical model based shape prediction from a combination of direct observations and various surrogates: Application to orthopaedic research. Medical Image Analysis 16(6):1156–1166
[17] van der Bom MJ, Bartels LW, Gounis MJ, Homan R, Timmer J, Viergever MA, Pluim JPW (2010) Robust initialization of 2D-3D image registration using the projection-slice theorem and phase correlation. Med Phys 37(4):1884–1892
[18] Burckhardt K, Székely G, Nötzli H, Hodler J, Gerber C (2005) Submillimeter measurement of cup migration in clinical standard radiographs. IEEE Trans Med Imag 24(5):676–688
[19] Burckhardt K, Dora C, Gerber C, Hodler J, Székely G (2006) Measuring orthopedic implant wear on standard radiographs with a precision in the 10 μm-range. Medical Image Analysis 10(4):520–529
[20] Chen Y, Medioni G (1992) Object modelling by registration of multiple range images. Image and Vision Computing 10(3):145–155
[21] Cho Y, Moseley DJ, Siewerdsen JH, Jaffray DA (2005) Accurate technique for complete geometric calibration of cone-beam computed tomography systems. Med Phys 32(4):968–983
[22] Claus BEH (2006) Geometry calibration phantom design for 3D imaging. In: Flynn MJ, Hsieh J (eds) SPIE Medical Imaging: Physics of Medical Imaging, SPIE, p 61422E
[23] Costa F, et al (2014) Economic study: a cost-effectiveness analysis of an intraoperative compared with a preoperative image-guided system in lumbar pedicle screw fixation in patients with degenerative spondylolisthesis. Spine 14(8):1790–1796
[24] Daly MJ, Siewerdsen JH, Cho YB, Jaffray DA, Irish JC (2008) Geometric calibration of a mobile C-arm for intraoperative cone-beam CT. Med Phys 35(5):2124–2136
[25] Dang H, Otake Y, Schafer S, Stayman JW, Kleinszig G, Siewerdsen JH (2012) Robust methods for automatic image-to-world registration in cone-beam CT interventional guidance. Med Phys 39(10):6484–6498

[26] Danilchenko A, Fitzpatrick JM (2011) General approach to first-order error prediction in rigid point registration. IEEE Trans Med Imag 30(3):679–693
[27] Dobbe JGG, Strackee SD, Schreurs AW, Jonges R, Carelsen B, Vroemen JC, Grimbergen CA, Streekstra GJ (2011) Computer-assisted planning and navigation for corrective distal radius osteotomy, based on pre- and intraoperative imaging. IEEE Trans Biomed Eng 58(1):182–190
[28] Dobbe JGG, Vroemen JC, Strackee SD, Streekstra GJ (2013) Corrective distal radius osteotomy: including bilateral differences in 3-D planning. Med Biol Engineering and Computing 51(7):791–797
[29] Dorgham OM, Laycock SD, Fisher MH (2012) GPU accelerated generation of digitally reconstructed radiographs for 2-D/3-D image registration. IEEE Trans Biomed Eng 59(9):2594–2603
[30] Eggert DW, Lorusso A, Fisher RB (1997) Estimating 3-D rigid body transformations: a comparison of four major algorithms. Mach Vis Appl 9(5/6):272–290
[31] Ershad M, Ahmadian A, Serej ND, Saberi H, Khoiy KA (2014) Minimization of target registration error for vertebra in image-guided spine surgery. International Journal of Computer Assisted Radiology and Surgery 9(1):29–38
[32] Faugeras OD, Hebert M (1986) The representation, recognition, and locating of 3-D objects. Int J Rob Res 5(3):27–52
[33] Fletcher R (1987) Practical methods of optimization; (2nd ed.). Wiley-Interscience
[34] Fleute M, Lavallée S, Julliard R (1999) Incorporating a statistically based shape model into a system for computer-assisted anterior cruciate ligament surgery. Medical Image Analysis 3(3):209–222
[35] Fürnstahl P, Székely G, Gerber C, Hodler J, Snedeker JG, Harders M (2012) Computer assisted reconstruction of complex proximal humerus fractures for preoperative planning. Medical Image Analysis 16(3):704–720
[36] Gill S, Abolmaesumi P, Fichtinger G, Boisvert J, Pichora DR, Borshneck D, Mousavi P (2012) Biomechanically constrained groupwise ultrasound to CT registration of the lumbar spine. Medical Image Analysis 16(3):662–674
[37] Gong RH, Özgür Güler, Kürklüoglu M, Lovejoy J, Yaniv Z (2013) Interactive initialization of 2D/3D rigid registration. Med Phys 20(12):121,911–1 – 121,911–14
[38] Gonschorek O, Hauck S, Spiegl U, Weiß T, Pätzold R, Bühren V (2011) O-arm based spinal navigation and intraoperative 3D-imaging: first experiences. European Journal of Trauma and Emergency Surgery 37(2):99–108
[39] Habets DF, Pollmann SI, Yuan X, Peters TM, Holdsworth DW (2009) Error analysis of marker-based object localization using a single-plane xrii. Med Phys 36(1):190–200
[40] Hamming NM, Daly MJ, Irish JC, Siewerdsen JH (2009) Automatic image-to-world registration based on x-ray projections in cone-beam CTguided interventions. Med Phys 36(5):1800–1812
[41] Hananouchi T, Saito M, Koyama T, Hagio K, Murase T, Sugano N, Yoshikawa H (2009) Tailor-made surgical guide based on rapid prototyping

technique for cup insertion in total hip arthroplasty. International Journal of Medical Robotics and Computer Assisted Surgery 5(2):164–169
[42] Hartley RI, Zisserman A (2000) Multiple View Geometry in Computer Vision. Cambridge University Press
[43] Haselbacher M, Sekyra K, Mayr E, Thaler M, Nogler M (2012) A new concept of a multiple-use screw-based shape-fitting plate in total knee arthroplasty. Bone Joint J 94-B(Supp-XLIV):65
[44] Heimann T, Meinzer H (2009) Statistical shape models for 3d medical image segmentation: A review. Medical Image Analysis 13(4):543–563
[45] Hofstetter R, Slomczykowski M, Sati M, Nolte LP (1999) Fluoroscopy as an imaging means for computer-assisted surgical navigation. Computer Aided Surgery 4(2):65–76
[46] Holly LT, Block O, Johnson JP (2006) Evaluation of registration techniques for spinal image guidance. J Neurosurg Spine 4(4):323–328
[47] Horn BKP (1987) Closed-form solution of absolute orientation using unit quaternions. Journal of the Optical Society of America A 4(4):629–642
[48] Hurvitz A, Joskowicz L (2008) Registration of a CT-like atlas to fluoroscopic X-ray images using intensity correspondences. International Journal of Computer Assisted Radiology and Surgery 3(6):493–504
[49] Jain AK, Mustafa T, Zhou Y, Burdette C, Chirikjian GS, Fichtinger G (2005) FTRAC-a robust fluoroscope tracking fiducial. Med Phys 32(10):3185–3198
[50] Jaramaz B, Eckman K (2006) 2D/3D registration for measurement of implant alignment after total hip replacement. In: Medical Image Computing and Computer-Assisted Intervention, pp 653–661
[51] Kang X, Armand M, Otake Y, Yau WP, Cheung PYS, Hu Y, Taylor RH (2014) Robustness and accuracy of feature-based single image 2-D-3-D registration without correspondences for image-guided intervention. IEEE Trans Biomed Eng 61(1):149–161
[52] Kantelhardt SR, Bock HC, Siam L, Larsen J, Burger R, Schillinger W, Bockermann V, Rohde V, Giese A (2010) Intra-osseous ultrasound for pedicle screw positioning in the subaxial cervical spine: an experimental study. Acta Neurochir 152(4):655–661
[53] de Kelft EV, Costa F, der Planken DV, Schils F (2012) A prospective multicenter registry on the accuracy of pedicle screw placement in the thoracic, lumbar, and sacral levels with the use of the O-arm imaging system and stealthstation navigation. Spine 37(25):E1580–E1587
[54] Kilian P, et al (2008) New visualization tools: computer vision and ultrasound for MIS navigation. International Journal of Medical Robotics and Computer Assisted Surgery 4(1):23–31
[55] Kim Y, Kim KI, hyeok Choi J, Lee K (2011) Novel methods for 3D postoperative analysis of total knee arthroplasty using 2D3D image registration. Clin Biomech 26(4):384–391
[56] Kobayashi K, Sakamoto M, Tanabe Y, Ariumi A, Sato T, Omori G, Koga Y (2009) Automated image registration for assessing three-dimensional align-

ment of entire lower extremity and implant position using bi-plane radiography. J Biomech 42(16):2818–2822

[57] Kowal J, Amstutz C, Langlotz F, Talib H, Ballester MG (2007) Automated bone contour detection in ultrasound B-mode images for minimally invasive registration in computer-assisted surgery an in vitro evaluation. International Journal of Medical Robotics and Computer Assisted Surgery 3(4):341–348

[58] Kozic N, Weber S, Büchler P, Lutz C, Reimers N, Ballester MÁG, Reyes M (2010) Optimisation of orthopaedic implant design using statistical shape space analysis based on level sets. Medical Image Analysis 14(3):265–275

[59] van de Kraats EB, Penney GP, Tomaževič D, van Walsum T, Niessen WJ (2005) Standardized evaluation methodology for 2-D3-D registration. IEEE Trans Med Imag 24(9):1177–1189

[60] Kunz M, Ma B, Rudan JF, Ellis RE, Pichora DR (2013) Image-guided distal radius osteotomy using patient- specific instrument guides. J Hand Surg Am 2013 Aug;38(8):1618-24 38(8):1618–1624

[61] Lang A, Mousavi P, Gill S, Fichtinger G, Abolmaesumi P (2012) Multi-modal registration of speckle-tracked freehand 3D ultrasound to CT in the lumbar spine. Medical Image Analysis 16(3):675–686

[62] Lehmann TM, Gönner C, Spitzer K (1999) Survey: Interpolation methods in medical image processing. IEEE Trans Med Imag 18(11):1049–1075

[63] Letta C, Schweizer A, , Fürnstahl P (2014) Quantification of contralateral differences of the scaphoid: A comparison of bone geometry in three dimensions. Anat Res Int

[64] Lin CC, et al (2013) Intervertebral anticollision constraints improve out-of-plane translation accuracy of a single-plane fluoroscopy-to-CT registration method for measuring spinal motion. Med Phys 40(3):031,912

[65] Livyatan H, Yaniv Z, Joskowicz L (2002) Robust automatic C-arm calibration for fluoroscopy-based navigation: a practical approach. In: Dohi T, et al (eds) Medical Image Computing and Computer-Assisted Intervention, pp 60–68

[66] Livyatan H, Yaniv Z, Joskowicz L (2003) Gradient-based 2D/3D rigid registration of fluoroscopic X-ray to CT. IEEE Trans Med Imag 22(11):1395–1406

[67] Lonner JH, John TK, Conditt MA (2010) Robotic arm-assisted UKA improves tibial component alignment a pilot study. Clin Orthop Relat Res 468(1):141–146.

[68] Lu S, et al (2009) A novel computer-assisted drill guide template for lumbar pedicle screw placement: a cadaveric and clinical study. International Journal of Medical Robotics and Computer Assisted Surgery 5(2):184–191

[69] Lu S, et al (2009) A novel patient-specific navigational template for cervical pedicle screw placement. Spine 34(26):E959–E964

[70] Ma B, Kunz M, Gammon B, Ellis RE, Pichora DR (2014) A laboratory comparison of computer navigation and individualized guides for distal radius osteotomy. International Journal of Computer Assisted Radiology and Surgery 9(4):713–724

[71] Mahfouz MR, Hoff WA, Komistek RD, Dennis DA (2003) A robust method for registration of three-dimensional knee implant models to two-dimensional fluoroscopy images. IEEE Trans Med Imag 22(12):1561–1574
[72] Maier-Hein L, Franz AM, dos Santos TR, Schmidt M, Fangerau M, Meinzer H, Fitzpatrick JM (2012) Convergent iterative closest-point algorithm to accomodate anisotropic and inhomogenous localization error. IEEE Trans Pattern Anal Machine Intell 34(8):1520–1532
[73] Mantwill F, Schulz AP, Faber A, Hollstein D, Kammal M, Fay A, Jürgens C (2005) Robotic systems in total hip arthroplasty - is the time ripe for a new approach? International Journal of Medical Robotics and Computer Assisted Surgery 1(4):8–19
[74] Markelj P, Tomaževič D, Pernuš F, Likar B (2008) Robust gradient-based 3-D/2-D registration of CT and MR to x-ray images. IEEE Trans Med Imag 27(12):1704–1714
[75] Markelj P, Tomaževič D, Likar B, Pernuš F (2012) A review of 3D/2D registration methods for image-guided interventions. Medical Image Analysis 16(3):642–661
[76] Mercier L, LangøT, Lindseth F, Collins DL (2005) A review of calibration techniques for freehand 3-D ultrasound systems. Ultrasound in Med Biol 31(4):449–471
[77] Moghari MH, Abolmaesumi P (2007) Point-based rigid-body registration using an unscented kalman filter. IEEE Trans Med Imag 26(12):1708–1728
[78] Momi ED, Cerveri P, Gambaretto E, Marchente M, Effretti O, Barbariga S, Gini G, Ferrigno G (2008) Robotic alignment of femoral cutting mask during total knee arthroplasty. International Journal of Computer Assisted Radiology and Surgery 3(5):413–419
[79] Mozes A, Chang TC, Arata L, Zhao W (2010) Three-dimensional A-mode ultrasound calibration and registration for robotic orthopaedic knee surgery. International Journal of Medical Robotics and Computer Assisted Surgery 6(1):91–101
[80] Najafi M, Afsham N, Abolmaesumi P, Rohling R (2014) A closed-form differential formulation for ultrasound spatial calibration: multi-wedge phantom. Ultrasound Med Biol 40(9):2231–2243
[81] Nakamura N, Sugano N, Nishii T, Miki H, Kakimoto A, Yamamura M (2009) Robot-assisted primary cementless total hip arthroplasty using surface registration techniques: a short-term clinical report. International Journal of Computer Assisted Radiology and Surgery 4(2):157–162
[82] Nogler M, Maurer H, Wimmer C, Gegenhuber C, Bach C, Krismer M (2001) Knee pain caused by a fiducial marker in the medial femoral condyle. Acta Orthop Scand 72(5):477–480
[83] Oertel MF, Hobart J, Stein M, Schreiber V, Scharbrodt W (2011) Clinical and methodological precision of spinal navigation assisted by 3D intraoperative O-arm radiographic imaging. J Neurosurg Spine 14(4):532–536

[84] Ohta N, Kanatani K (1998) Optimal estimation of three-dimensional rotation and reliability evaluation. In: Computer Vision ECCV'98, LNCS, vol 1406/1998, pp 175–187

[85] Oka K, Moritomo H, Goto A, Sugamoto K, Yoshikawa H, Murase T (2008) Corrective osteotomy for malunited intra-articular fracture of the distal radius using a custom-made surgical guide based on three-dimensional computer simulation: case report. J Hand Surg Am 33(6):835–840

[86] Okada T, Iwasaki Y, Koyama T, Sugano N, Chen Y, Yonenobu K, Sato Y (2009) Computer-assisted preoperative planning for reduction of proximal femoral fracture using 3-d-ct data. IEEE Trans Biomed Eng 56(3):749–759

[87] Otake Y, Armand M, Armiger RS, Kutzer MDM, Basafa E, Kazanzides P, Taylor RH (2012) Intraoperative image-based multiview 2d/3d registration for image-guided orthopaedic surgery: Incorporation of fiducial-based c-arm tracking and gpu-acceleration. IEEE Trans Med Imag 31(4):948–962

[88] Otake Y, Schafer S, Stayman JW, Zbijewski W, Kleinszig G, Graumann R, Khanna AJ, Siewerdsen JH (2012) Automatic localization of vertebral levels in x-ray fluoroscopy using 3D-2D registration: a tool to reduce wrong-site surgery. Phys Med Biol 57(17):5485–5508

[89] Otake Y, Wang AS, Stayman JW, Uneri A, Kleinszig G, Vogt S, Khanna AJ, Gokaslan ZL, Siewerdsen JH (2013) Robust 3D-2D image registration: application to spine interventions and vertebral labeling in the presence of anatomical deformation. Phys Med Biol 58(23):8535–8553

[90] Otomaru I, Nakamoto M, Kagiyama Y, Takao M, Sugano N, Tomiyama N, Tada Y, Sato Y (2012) Automated preoperative planning of femoral stem in total hip arthroplasty from 3D CT data: Atlas-based approach and comparative study. Medical Image Analysis 16(2):415–426

[91] Pawiro SA, Markelj P, Pernus F, Gendrin C, Figl M, Weber C, Kainberger F, Nobauer-Huhmann I, Bergmeister H, Stock M, Georg D, Bergmann H, Birkfellner W (2011) Validation for 2D/3D registration I: A new gold standard data set. Med Phys 38(3):1481–1490

[92] Penney GP, Weese J, Little JA, Desmedt P, Hill DLG, Hawkes DJ (1998) A comparison of similarity measures for use in 2D-3D medical image registration. IEEE Trans Med Imag 17(4):586–595

[93] Penney GP, Batchelor PG, Hill DLG, Hawkes DJ, Weese J (2001) Validation of a two-to three-dimensional registration algorithm for aligning preoperative CT images and intraoperative fluoroscopy images. Med Phys 28(6):1024–1032

[94] Penney GP, Barratt DC, Chan CSK, Slomczykowski M, Carter TJ, Edwards PJ, Hawkes DJ (2006) Cadaver validation of intensity-based ultrasound to CT registration. Medical Image Analysis 10(3):385–395

[95] Penney GP, Edwards PJ, Hipwell JH, Slomczykowski M, Revie I, Hawkes DJ (2007) Postoperative calculation of acetabular cup position using 2-D-3-D registration. IEEE Trans Biomed Eng 54(7):1342–1348

[96] Petermann J, Kober R, Heinze R, Frölich JJ, Heeckt PF, Gotzen L (2000) Computer-assisted planning and robot-assisted surgery in anterior cruciate ligament reconstruction. Operative Techniques in Orthopaedics 10(1):50–55
[97] Quiñones-Hinojosa A, Kolen ER, Jun P, Rosenberg WS, Weinstein PR (2006) Accuracy over space and time of computer-assisted fluoroscopic navigation in the lumbar spine in vivo. J Spinal Disord Tech 2006 Apr;19(2):109-13 19(2):109–113
[98] Radermacher K, Portheine F, Anton M, Zimolong A, Kaspers G, Rau G, Staudte HW (1998) Computer assisted orthopaedic surgery with image based individual templates. Clin Orthop Relat Res Sep.(354):28–38
[99] Rajamani KT, Styner MA, Talib H, Zheng G, Nolte L, Ballester MÁG (2007) Statistical deformable bone models for robust 3D surface extrapolation from sparse data. Medical Image Analysis 11(2):99–109
[100] Rasoulian A, Abolmaesumi P, Mousavi P (2012) Feature-based multibody rigid registration of CT and ultrasound images of lumbar spine. Med Phys 39(6):3154–3166
[101] Richter M, Zech S (2008) 3D imaging (ARCADIS)-based computer assisted surgery (CAS) guided retrograde drilling in osteochondritis dissecans of the talus. Foot Ankle Int 29(12):1243–1248
[102] Rieger M, Gabl M, Gruber H, Jaschke WR, Mallouhi A (2005) CT virtual reality in the preoperative workup of malunited distal radius fractures: preliminary results. Eur Radiol 4(15):792–797
[103] Rodriguez F, et al (2005) Robotic clinical trials of uni-condylar arthroplasty. International Journal of Medical Robotics and Computer Assisted Surgery 1(4):20–28
[104] Rueckert D, Sonoda LI, Hayes C, Hill DLG, Leach MO, Hawkes DJ (1999) Non-rigid registration using free-form deformations: Application to breast MR images. IEEE Trans Med Imag 18(8):712–721
[105] Rusinkiewicz S, Levoy M (2001) Efficient variants of the ICP algorithm. In: International Conference on 3D Digital Imaging and Modeling, pp 145–152
[106] Russakoff DB, Rohlfing T, Adler JR Jr, Maurer CR Jr (2005) Intensity-based 2D-3D spine image registration incorporating a single fiducial marker. Academic Radiology 12(1):37–50
[107] Schafer S, et al (2011) Mobile C-arm cone-beam CT for guidance of spine surgery: Image quality, radiation dose, and integration with interventional guidance. Med Phys 38(8):4563–4574
[108] Schuler B, Fritscher KD, Kuhn V, Eckstein F, Link TM, Schubert R (2010) Assessment of the individual fracture risk of the proximal femur by using statistical appearance models. Med Phys 37(6):2560–2571
[109] Schulz AP, Seide K, Queitsch C, von Haugwitz A, Meiners J, Kienast B, Tarabolsi M, Kammal M, Jürgens C (2007) Results of total hip replacement using the Robodoc surgical assistant system: clinical outcome and evaluation of complications for 97 procedures. International Journal of Medical Robotics and Computer Assisted Surgery 3(4):301–306

[110] Schumann S, Nolte LP, Zheng G (2012) Determination of pelvic orientation from sparse ultrasound data for THA operated in the lateral position. International Journal of Medical Robotics and Computer Assisted Surgery 8(1):107–113
[111] Schweizer A, Fürnstahl P, Harders M, Székely G, Nagy L (2010) Complex radius shaft malunion: Osteotomy with computer-assisted planning. HAND 5:171–178
[112] Shamir RR, Joskowicz L, Spektor S, Shoshan Y (2009) Localization and registration accuracy in image guided neurosurgery: a clinical study. International Journal of Computer Assisted Radiology and Surgery 4(1):45–52
[113] Shoham M, Burman M, Zehavi E, Joskowicz L, Batkilin E, Kunicher Y (2003) Bone-mounted miniature robot for surgical procedures: Concept and clinical applications. IEEE Trans Robot Automat 19(5):893–901
[114] Shoham M, et al (2007) Robotic assisted spinal surgery from concept to clinical practice. Computer Aided Surgery 12(2):105–115
[115] Smith EJ, Al-Sanawi H, Gammon B, John PS, Pichora DR, Ellis RE (2012) Volume slicing of cone-beam computed tomography images for navigation of percutaneous scaphoid fixation. International Journal of Computer Assisted Radiology and Surgery 7(3):433–444
[116] Smith JR, Riches PE, Rowe PJ (2014) Accuracy of a freehand sculpting tool for unicondylar knee replacement. International Journal of Medical Robotics and Computer Assisted Surgery 10(2):162–169
[117] Stindel E, Briard JL, Merloz P, Plaweski S, Dubrana F, Lefevre C, Troccaz J (2002) Bone morphing: 3D morphological data for total knee arthroplasty. Computer Aided Surgery 7(3):156–168
[118] Stöckle U, Schaser K, König B (2007) Image guidance in pelvic and acetabular surgery-expectations, success and limitations. Injury 38(4):450–462
[119] Sugano N (2013) Computer-assisted orthopaedic surgery and robotic surgery in total hip arthroplasty. Clin Orthop Surg 5(1):1–9
[120] Talib H, Peterhans M, Garća J, Styner M, Ballester MAG (2011) Information filtering for ultrasound-based real-time registration. IEEE Trans Biomed Eng 58(3):531–540
[121] Tate PM, Lachine V, Fu L, Croitoru H, Sati M (2001) Performance and robustness of automatic fluoroscopic image calibration in a new computer assisted surgery system. In: Medical Image Computing and Computer-Assisted Intervention, pp 1130–1136
[122] Tensho K, Kodaira H, Yasuda G, Yoshimura Y, Narita N, Morioka S, Kato H, Saito N (2011) Anatomic double-bundle anterior cruciate ligament reconstruction, using CT-based navigation and fiducial markers. Knee Surg Sports Traumatol Arthrosc 2011 Mar;19(3):378-83 19(3):378–383
[123] Tomaževič D, Likar B, Pernuš F (2004) "gold standard" data for evaluation and comparison of 3D/2D registration methods. Computer Aided Surgery 9(4):137–144
[124] Tomaževič D, Likar B, Slivnik T, Pernuš F (2003) 3-D/2-D registration of CT and MR to X-ray images. IEEE Trans Med Imag 22(11):1407–1416

[125] Tomaževič D, Likar B, Pernuš F (2006) 3-D/2-D registration by integrating 2-D information in 3-D. IEEE Trans Med Imag 25(1):17–27
[126] Tornai GJ, Pappasa GC (2012) Fast DRR generation for 2D to 3D registration on GPUs. Med Phys 39(8):4795–4799
[127] Tsai TY, Lu TW, Chen CM, Kuo MY, Hsu HC (2010) A volumetric model-based 2D to 3D registration method for measuring kinematics of natural knees with single-plane fluoroscopy. Med Phys 37(3):1273–1284
[128] Umeyama S (1991) Least-squares estimation of transformation parameters between two point patterns. IEEE Trans Pattern Anal Machine Intell 13(4):376–380
[129] Uneri A, Otake Y, Wang AS, Kleinszig G, Vogt S, Khanna AJ, Siewerdsen JH (2014) 3D2D registration for surgical guidance: effect of projection view angles on registration accuracy. Phys Med Biol 59(2):271–287
[130] Varnavas A, Carrell T, Penney GP (2013) Increasing the automation of a 2D-3D registration system. IEEE Trans Med Imag 32(2):387–399
[131] Vercauteren T, Pennec X, Perchant A, Ayache N (2009) Diffeomorphic demons: Efficient non-parametric image registration. NeuroImage 45(1, Supplement 1):S61 – S72
[132] Walker MW, Shao L, Volz RA (1991) Estimating 3-D location parameters using dual number quaternions. CVGIP: Image Understanding 54(3):358–367
[133] Wei W, Schön N, Dannenmann T, Petzold R (2011) Determining the position of a patient reference from C-Arm views for image guided navigation. International Journal of Computer Assisted Radiology and Surgery 6(2):217–227
[134] Weil YA, Liebergall M, Mosheiff R, Singer SB, Joskowicz L, Khoury A (2011) Assessment of two 3-d fluoroscopic systems for articular fracture reduction: a cadaver study. International Journal of Computer Assisted Radiology and Surgery 6(5):685–692
[135] Wein W, Brunke S, Khamene A, Callstrom MR, Navab N (2008) Automatic CT-ultrasound registration for diagnostic imaging and image-guided intervention. Medical Image Analysis 12:577–585
[136] West J, et al (1997) Comparison and evaluation of retrospective intermodality brain image registration techniques. Journal of Computer Assisted Tomography 4(4):554–568
[137] Whitmarsh T, Humbert L, Craene MD, Barquero LMDR, Frangi AF (2011) Reconstructing the 3D shape and bone mineral density distribution of the proximal femur from dual-energy X-ray absorptiometry. IEEE Trans Med Imag 12(30):2101–2114
[138] Wiles AD, Likholyot A, Frantz DD, Peters TM (2008) A statistical model for point-based target registration error with anisotropic fiducial localizer error. IEEE Trans Med Imag 27(3):378–390
[139] Wing JM (2006) Computational thinking. Commun ACM 49(3):33–35
[140] Xie W, Franke J, Chen C, Grützner PA, Schumann S, Nolte L, Zheng G (2014) Statistical model-based segmentation of the proximal femur in digital

antero-posterior (AP) pelvic radiographs. International Journal of Computer Assisted Radiology and Surgery 9(2):165–176
[141] Yan CXB, Goulet B, Pelletier J, Chen SJS, Tampieri D, Collins DL (2011) Towards accurate, robust and practical ultrasound-CT registration of vertebrae for image-guided spine surgery. International Journal of Computer Assisted Radiology and Surgery 6(4):523–537
[142] Yan CXB, Goulet B, Chen SJ, Tampieri D, Collins DL (2012) Validation of automated ultrasound-ct registration of vertebrae. International Journal of Computer Assisted Radiology and Surgery 7(4):601–610
[143] Yan CXB, Goulet B, Tampieri D, Collins DL (2012) Ultrasound-CT registration of vertebrae without reconstruction. International Journal of Computer Assisted Radiology and Surgery 7(6):901–909
[144] Yaniv Z (2009) Localizing spherical fiducials in c-arm based cone-beam CT. Med Phys 36(11):4957–4966
[145] Yaniv Z (2010) Evaluation of spherical fiducial localization in C-arm cone-beam CT using patient data. Med Phys 37(10):5298–5305
[146] Yaniv Z, Joskowicz L (2005) Precise robot-assisted guide positioning for distal locking of intramedullary nails. IEEE Trans Med Imag 24(5):624–635
[147] Zeng X, Wang C, Zhou H, Wei S, Chen X (2014) Low-dose three-dimensional reconstruction of the femur with unit free-form deformation. Med Phys 41(8):081,911
[148] Zhang YZ, Chen B, Lu S, Yang Y, Zhao JM, Liu R, Li YB, Pei GX (2011) Preliminary application of computer-assisted patient-specific acetabular navigational template for total hip arthroplasty in adult single development dysplasia of the hip. International Journal of Medical Robotics and Computer Assisted Surgery 7(4):469–474
[149] Zhang Z (1994) Iterative point matching for registration of free-form curves and surfaces. International Journal of Computer Vision 13(2):119–152
[150] Zheng G, Zhang X (2009) Robust automatic detection and removal of fiducial projections in fluoroscopy images: An integrated solution. Med Eng Phys 31(5):571–580
[151] Zheng G, Zhang X (2010) Computer assisted determination of acetabular cup orientation using 2D-3D image registration. International Journal of Computer Assisted Radiology and Surgery 5(5):437–447
[152] Zheng G, Gollmer S, Schumann S, Dong X, Feilkas T, Ballester MÁG (2009) A 2D/3D correspondence building method for reconstruction of a patient-specific 3D bone surface model using point distribution models and calibrated X-ray images. Medical Image Analysis 13(6):883–899
[153] Zheng G, Zhang X, Steppacher SD, Murphy SB, Siebenrock K, Tannast M (2009) Hipmatch: An object-oriented cross-platform program for accurate determination of cup orientation using 2D-3D registration of single standard X-ray radiograph and a CT volume. Computer Methods and Programs in Biomedicine 95(3):236–248
[154] Zheng G, Schumann S, Ballester MÁG (2010) An integrated approach for reconstructing a surface model of the proximal femur from sparse input data

and a multi-resolution point distribution model: an in vitro study. International Journal of Computer Assisted Radiology and Surgery 5(1):99–107

[155] Zheng G, von Recum J, Nolte L, Grützner PA, Steppacher SD, Franke J (2012) Validation of a statistical shape model-based 2D/3D reconstruction method for determination of cup orientation after THA. International Journal of Computer Assisted Radiology and Surgery 7(2):225–231